

Electronic structure from conditional probabilities

Ryan J. McCarty,¹ Dennis Perchak,¹ Ryan Pederson,² Robert Evans,³ Yiheng Qiu,² Steven R. White,² and Kieron Burke^{1,2,*}

¹Department of Chemistry, University of California, Irvine, CA, 92697

²Department of Physics and Astronomy, University of California, Irvine, CA, 92697

³H H Wills Physics Laboratory, University of Bristol, Bristol BS8 1TL, UK

(Dated: Friday 11th October, 2024)

Accurate ground-state energies are the focus of most electronic structure calculations. Such energies can, in principle, be extracted from a sequence of density functional calculations of conditional probabilities (CP-DFT), *without* approximating the energy directly. Simple CP approximations yield usefully accurate results for a broad range of systems: two-electron ions, the hydrogen dimer, and the uniform gas at all temperatures. CP-DFT has no self-interaction error for one electron, and correctly dissociates H₂, both major challenges in standard density functional theory. Orbital free CP-DFT may be ideal for warm dense matter simulations.

Modern electronic structure calculations usually focus on finding accurate ground-state energies, as so many properties of a molecule or a material depend on this ability [1]. Wavefunction-based methods, such as coupled-cluster theory [2, 3] or quantum Monte Carlo (QMC) [4, 5], directly yield energies. Kohn-Sham (KS) density functional theory (DFT) [6] incorporates all unknown aspects of the many-electron problem into the exchange-correlation energy, which must be approximated as a functional of spin densities. Literally hundreds of distinct approximations to the exchange-correlation (XC) energy are available in most standard codes [7], reflecting the tremendous difficulty in finding general, accurate approximations to the energy directly. Recently, KS-DFT at finite temperatures, based on the Mermin theorem [8], has been tremendously successful in simulations of warm dense matter [9, 10].

But XC energies are entirely determined by pair densities, the joint probability density for finding electrons at two points. The pair density of a ground-state wavefunction can always be written as

$$P(\mathbf{r}, \mathbf{r}') = n(\mathbf{r}) \tilde{n}_{\mathbf{r}}(\mathbf{r}'), \quad (1)$$

where $n(\mathbf{r})$ is the single particle density, and $\tilde{n}_{\mathbf{r}}(\mathbf{r}')$ is the conditional probability (CP) density of finding an electron at \mathbf{r}' , given an electron at \mathbf{r} . The standard exact KS potential of DFT, $v_s[n](\mathbf{r})$, is defined to yield $n(\mathbf{r})$ in an effective fermionic non-interacting problem [11]. Similarly, if it exists, for each \mathbf{r} , the conditional probability KS potential (CPKS), $v_s[\tilde{n}_{\mathbf{r}}](\mathbf{r}')$ yields $\tilde{n}_{\mathbf{r}}(\mathbf{r}')$ from such a KS calculation with $N - 1$ electrons. Because standard KS-DFT calculations usually yield highly accurate densities [12], an accurate approximation to the CPKS potential should yield highly accurate XC energies.

Under many circumstances (such as well-separated points or higher temperatures), the CP potential is simply approximated by adding $1/|\mathbf{r} - \mathbf{r}'|$ to the external potential, i.e., the repulsion due to the missing electron as if it were a classical point particle. We call this a blue electron, to denote an electron distinguishable from all others, recalling the Percus test particle procedure used in classical

statistical mechanics [13]. However, at small separations, the pair density must satisfy the electron-electron cusp condition [14], which implies adding only 1/2 this potential (the 2 is due to the reduced mass). We use a rudimentary interpolation between these limits in our calculations.

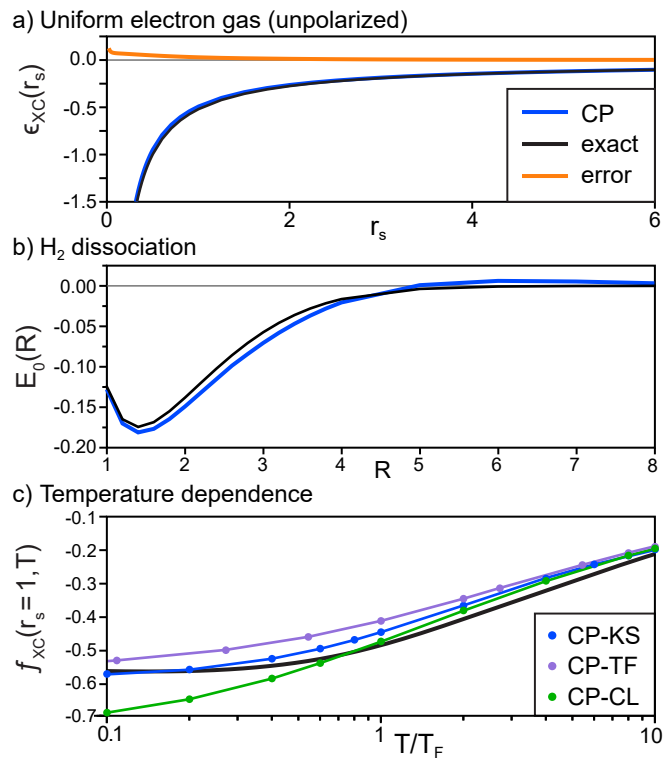


FIG. 1. CP (blue) and exact (black) energies in various systems: (a) XC energy per particle in uniform gas at increasing Wigner–Seitz radii (r_s) and $T = 0K$, (b) binding energy curve for H₂, and (c) XC free energy per particle at $r_s = 1$ as a function of reduced temperature (T_F is the Fermi temperature) for three different approximations: KS (Kohn-Sham), TF (Thomas-Fermi), and CL (classical)). In (a), exact from Ref. [15] and in (c) to Karasiev et al. [16]. Hartree atomic units are used throughout.

Representative results are shown in Fig 1. For the simplest system, the uniform electron gas at zero temperature, our CP potential interpolation is extremely accurate (we chose our interpolation with this in mind). In this panel only, we have added an additional strong repulsion for $r_s < 1$, to ensure recovery of the exchange limit. The middle panel shows results for the H_2 binding curve, where the inclusion of the electron-electron cusp is vital. Unlike semi-local DFT, CP-DFT dissociates the molecule correctly, remaining spin-unpolarized throughout. The bottom panel (c) shows that CP can be used at all temperatures T . As T is raised from very low to very high (on the scale of the Fermi energy), the CP-DFT error for r_s never exceeds 20% and vanishes in the high temperature limit. Moreover, results of orbital-free Thomas-Fermi CP calculations, and even a classical CP calculation, agree reasonably with both KS-CP and the accurate results for all $T > T_F$, the Fermi temperature.

Theory: We consider non-relativistic purely electronic problems, and use Hartree atomic units throughout. The pair density is extractable from the exact wavefunction:

$$P^\lambda(\mathbf{r}_1, \mathbf{r}_2) = N(N-1) \sum_{\sigma_1 \sigma_2} \int d3 \dots dN |\Psi^\lambda(1 \dots N)|^2. \quad (2)$$

where N is the number of electrons and Ψ^λ is the ground-state wavefunction. Here 1 is shorthand for both \mathbf{r}_1 and σ_1 , the spatial and spin indices. The λ -dependence is the usual coupling constant in KS DFT, where the repulsion is multiplied by λ but the one-body potential $v^\lambda(\mathbf{r})$ is adjusted to keep the ground-state density $n(\mathbf{r})$ fixed [17]. The standard wavefunction and original potential is at $\lambda = 1$; the KS wavefunction and potential are at $\lambda = 0$. We need this to extract the exact XC energy:

$$E_{XC} = \frac{1}{2} \int_0^1 d\lambda \int d^3r \int d^3r' \frac{n(\mathbf{r}) [\tilde{n}_\mathbf{r}^\lambda(\mathbf{r}') - n(\mathbf{r})]}{|\mathbf{r} - \mathbf{r}'|}, \quad (3)$$

with $\tilde{n}_\mathbf{r}^\lambda(\mathbf{r}') - n(\mathbf{r})$ being the λ -dependent XC hole, defined via the λ -dependent generalization of Eq. 1. Setting $\lambda = 1$ in Eq. 3 yields U_{XC} , the potential contribution to XC.

We next denote $v^\lambda[n](\mathbf{r})$ as the unique one-body potential that has $n(\mathbf{r})$ as its ground-state for electron repulsion $\lambda/|\mathbf{r} - \mathbf{r}'|$. Then the conditional probability potential is defined as

$$\tilde{v}^\lambda(\mathbf{r}'|\mathbf{r}) = v[\tilde{n}_\mathbf{r}^\lambda](\mathbf{r}') = v[n](\mathbf{r}') + \Delta\tilde{v}_\mathbf{r}^\lambda[n](\mathbf{r}'), \quad (4)$$

being the unique potential whose exact ground-state density for Coulomb interacting electrons yields the exact λ -dependent CP density and hence the exact XC energy. The CP-KS potential is found self-consistently as usual:

$$\tilde{v}_s^\lambda(\mathbf{r}'|\mathbf{r}) = v_s[\tilde{n}_\mathbf{r}^\lambda](\mathbf{r}') = \tilde{v}^\lambda(\mathbf{r}'|\mathbf{r}) + v_{HXC}[\tilde{n}_\mathbf{r}^\lambda](\mathbf{r}'), \quad (5)$$

where v_{HXC} is the usual Hartree-XC potential [1]. Thus knowledge of the CP correction potential, $\Delta\tilde{v}_\mathbf{r}^\lambda[n](\mathbf{r}')$ in

Eq. 4, allows a self-consistent KS calculation for the CP density which is, in principle, exact. Uniqueness of the CP potential is guaranteed by the HK theorem. As $n_\mathbf{r}^\lambda(\mathbf{r}')$ is non-negative, normalized to $N - 1$, and found from a wavefunction, it is likely to be in the standard space of densities, for which we routinely assume KS potentials exist [18, 19].

All the above equations are for pure density functionals, and their analogs for spin-density functionals are straightforward (but cumbersome). Decades of research in DFT can be applied to the study of CP densities and potentials, yielding many exact conditions. Here we mention a few. At $\lambda = 0$, we have the exchange limit. Because the exchange hole is never positive,

$$\tilde{n}_\mathbf{r}^{\lambda=0}(\mathbf{r}') \leq n(\mathbf{r}'). \quad (6)$$

The CP densities satisfy a complementarity principle:

$$\tilde{n}_\mathbf{r}^\lambda(\mathbf{r}') = \frac{n(\mathbf{r})}{n(\mathbf{r}')} \tilde{n}_{\mathbf{r}'}^\lambda(\mathbf{r}), \quad (7)$$

which is Bayesian, and may be amenable to modern machine-learning methods. The electron coalescence cusp condition requires

$$\left. \frac{\partial \tilde{n}_\mathbf{r}^\lambda(\mathbf{r}, u)}{\partial u} \right|_{u=0} = \lambda \tilde{n}_\mathbf{r}^\lambda(\mathbf{r}), \quad (8)$$

where $\mathbf{u} = \mathbf{r}' - \mathbf{r}$ and the left-hand side has been spherically averaged over $\mathbf{r} + \mathbf{u}$ [20]. For $N = 1$, $n_\mathbf{r}^\lambda(\mathbf{r}') = 0$, so a CP calculation suffers no self-interaction error [21]. If $N = 2$, the CP density is for just one electron:

$$\tilde{\phi}_\mathbf{r}^\lambda(\mathbf{r}') = \sqrt{\tilde{n}_\mathbf{r}^\lambda(\mathbf{r}')} = \sqrt{\frac{2}{n(\mathbf{r})}} \Psi^\lambda(\mathbf{r}, \mathbf{r}'), \quad (9)$$

yielding

$$\tilde{v}_s^\lambda(\mathbf{r}'|\mathbf{r}) - \epsilon_\mathbf{r}^\lambda = \frac{1}{2} \frac{\nabla'^2 \Psi^\lambda(\mathbf{r}, \mathbf{r}')}{\Psi^\lambda(\mathbf{r}, \mathbf{r}')}, \quad (10)$$

where $\epsilon_\mathbf{r}^\lambda$ is the eigenvalue of the CPKS potential. Because the wavefunction satisfies the Schrödinger equation, we find

$$\Delta\tilde{v}_s^\lambda(\mathbf{r}'|\mathbf{r}) + \Delta\tilde{v}_s^\lambda(\mathbf{r}|\mathbf{r}') = \frac{\lambda}{|\mathbf{r} - \mathbf{r}'|} - E^\lambda, \quad (11)$$

where $\Delta\tilde{v}_s^\lambda(\mathbf{r}'|\mathbf{r}) = \tilde{v}_s^\lambda(\mathbf{r}'|\mathbf{r}) - v^\lambda[n](\mathbf{r}') - \epsilon_\mathbf{r}^\lambda$, and $n(\mathbf{r})$ is the exact density.

Approximations: Definitions are useful, but do not lead to practical approximations. To perform a CP-DFT calculation, we need a general-purpose approximation to the CP potential, $\Delta\tilde{v}_\mathbf{r}^\lambda(\mathbf{r}')$. To create a theory for these potentials, we use technology from Ref. [22], but generalized to arbitrary positive λ . The starting point is

$$\Psi^\lambda(1 \dots N) = \sqrt{\frac{n(\mathbf{r}_1)}{N}} \tilde{\Psi}_\mathbf{r}^\lambda(2 \dots N). \quad (12)$$

Note that $\tilde{\Psi}_r^\lambda$ is not antisymmetric under interchange of the electrons, but it is uniquely defined by Eq. 12, and n_r^λ is its density (it is antisymmetric under interchange of coordinates 2 to N). Ref. [22] focused on finding an exact effective equation for the density $n(\mathbf{r})$, but it also yields an apparent Schrödinger equation for $\tilde{\Psi}_r$ with Hamiltonian:

$$\tilde{H}^\lambda = H^\lambda(2 \dots N) + \sum_{j=2}^N \frac{\lambda}{|\mathbf{r} - \mathbf{r}_j|} + v_{nuc}^\lambda(2 \dots N|\mathbf{r}) \quad (13)$$

where $H^\lambda(2 \dots N)$ is the sum of the kinetic and one-body potential energies of these electrons in potential $v(\mathbf{r}_j)$, and the 'nuclear potential' actually includes gradients of $\tilde{\Psi}^\lambda$ with respect to \mathbf{r} . Unlike a standard Schrödinger equation, this is *not* an eigenvalue equation that you solve with given boundary conditions. Instead, it is a differential equation satisfied by $\tilde{\Psi}^\lambda$, defined by Eq. 12. This is an example of the exact factorization technique that has become popular for studying nuclear dynamics, but can also be applied to the pure electronic problem [23]. In that case, it is known that the conditional wavefunctions are not always the lowest eigenstate if one treats this as an eigenvalue problem [24]. Worse still, the appearance of the nuclear many-body potential, depending on $N - 1$ coordinates simultaneously, means that the usual theorems of DFT cannot be applied.

While we cannot use this analysis to find $\tilde{v}_s^\lambda(\mathbf{r}'|\mathbf{r})$ exactly, we can easily use it to make a good approximation. Drop the nuclear potential, and consider the corresponding differential equation, which now matches a standard $N - 1$ -electron problem, once we identify

$$\Delta\tilde{v}_r^\lambda[n](\mathbf{r}') \approx \frac{\lambda}{|\mathbf{r} - \mathbf{r}'|}. \quad (14)$$

We call this a blue electron approximation, as it comes from treating one electron as distinguishable from all others (painted blue), and so adds a Coulomb repulsion to the one-body potential. This becomes exact for large r , as Ref. [22] shows $\tilde{\Psi}_r$ collapses to the $N - 1$ -electron ground state. As we shall see, it is also exact in the high temperature, classical, and even strongly correlated limits. But a pure blue approximation must fail at small separations, as it yields a cusp that is too large by a factor of 2. Instead, we interpolate with a local density approximation

$$\Delta\tilde{v}_r^\lambda[n](\mathbf{r}') \approx \frac{\lambda}{2|\mathbf{r} - \mathbf{r}'|} (1 + \text{Erf} \left(\frac{|\mathbf{r} - \mathbf{r}'|}{r_s(n(\mathbf{r}))} \right)), \quad (15)$$

where $r_s = (3/(4\pi n))^{1/3}$ is the Wigner-Seitz radius at the reference point. Fig. 1 (a) and (b), use this approximation combined with standard DFT approximations for v_{XC} , Fig. 1(c) uses Eq. (14).

Uniform electron gas: The N -electron density is trivially a constant, and the one-body potential vanishes. The CP calculation is for $N - 1$ electrons in a KS potential:

$$v_s(r) = \Delta\tilde{v}(r) + \int d^3r' \frac{\tilde{n}(\mathbf{r}') - n_0}{|\mathbf{r} - \mathbf{r}'|} + v_{XC}^{\text{LDA}}[\tilde{n}](\mathbf{r}), \quad (16)$$

where $n_0 = N/V$ and

$$\Delta\tilde{v}(r) = \Delta\tilde{v}_0(r) + A(r_s)e^{-r^2/2\sigma(r_s)^2}. \quad (17)$$

The second term is an added potential that ensures recovery of the correct high-density limit, i.e., makes the blue calculation yield the simple $n^{4/3}$ exchange energy in this limit. If we run the calculation for many r_s values, we can perform the adiabatic connection integral by integrating over r_s , so we need only $\lambda = 1$. For the XC potential, we use a standard parameterization [25]. The strength and range parameters of the added Gaussian potential are fitted to the uniform gas XC energy for $r_s = 0.02$, i.e., where exchange dominates. The calculation is actually performed in a finite sphere. The density is found self-consistently using Fermi-surface smearing with a temperature of 5% of the Fermi energy. Imposing zero density flux through the surface of the sphere minimizes boundary effects. We solve both the neutral and blue-electron systems in the same way, so as to maximize cancellation of boundary effects. We find $N = 512$ is sufficient for convergence with respect to particle number/system size. Further details of the solution method and the Gaussian potential parameterization will be described in a forthcoming paper.

Fig. 2 shows the hole density compared to that given by the parameterization of the uniform gas XC hole [26]. The agreement is very good, with the lowest accuracy from the on-top region, which has very little weight in the XC energy.

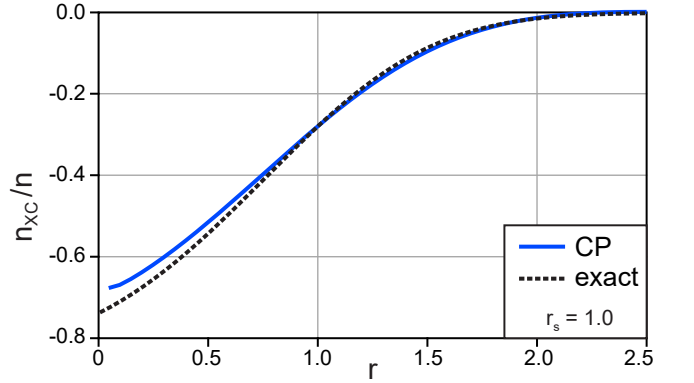


FIG. 2. Normalized XC hole densities for the uniform gas at $r_s = 1$, both CP (blue) and as parameterized for the uniform electron gas [26] (black).

Atoms and molecules: We applied our approximate formula to highly accurate calculations of 2-electron systems. These calculations were done using a new type of basis function called gausslets [27, 28] which is tailored for density matrix renormalization group calculations [29] and based on wavelets. While gausslets are basis functions, in their use they resemble a variable-spaced real-space grid. In particular, the two-electron Hamiltonian terms have only two indices, V_{ij} , unlike the four indices needed in a standard

basis. The simple nature of the Hamiltonian and its grid-like structure make CP calculations particularly easy to implement. For example, a blue electron sitting at a point in space sits on a gausslet, i , located at its reference, \mathbf{r}_i . The repulsive one-electron potential of Eq. (14) at i is simply row i of V_{ij} . Integration likewise turns into point-wise sums. The current implementation includes recent innovations, such as incorporating a Gaussian basis in addition to the gausslets to better describe atomic core behavior, further described in a forthcoming work. The calculations used no more than 2000 gausslets with errors in total energies for $Z = 1$ and $Z = 2$ below 0.1 mH. For any two electron system, fixing one blue electron leaves only one other electron left, so to find the associated conditional probability, we find the ground state of an $N \times N$ matrix with the Lanczos algorithm [30] and repeat this N times. We expect gausslets to make an excellent choice of basis for CP calculations of N -electron systems. Regardless of the basis, CP calculations are receptive to parallel computing, as each value of \mathbf{r} and λ can be computed independently.

We present results for 2-electron ions in Table I. We have performed the double integral over \mathbf{r} and \mathbf{r}' , to find the potential contribution to correlation, denoted U_C . The virial theorem for atoms (relating the total energy to total kinetic energy, $E = -T$) allows us to deduce a corresponding value of E_C , without needing to perform the adiabatic connection. For He, the correlation energy error is just 8 mH, and is only 20% for both U_C and E_C . As $Z \rightarrow \infty$, the CP calculation correctly yields a finite value, keeping precisely the same 8 mH overestimate (in magnitude).

Z	E_X	V_{ee}^{CP}	U_C^{CP}	U_C^{Exact}	virial E_C^{CP}	E_C^{Exact}
1.0	-0.3810	0.2828	-0.0982	-0.0698	-0.0562	-0.0420
2.0	-1.0245	0.9294	-0.0951	-0.0786	-0.0503	-0.0421
3.0	-1.6510	1.5518	-0.0992	-0.0832	-0.0515	-0.0435
4.0	-2.2766	2.1748	-0.1017	-0.0857	-0.0523	-0.0443
6.0	-3.5270	3.4225	-0.1045	-0.0881	-0.0534	-0.0452

TABLE I. Results for 2-electron Helium-like ions, where the virial E_C^{CP} is derived from the virial theorem for atoms using exact T_s from Ref. [31].

However, this virial trick only works for Coulomb-interacting atoms and molecules at equilibrium. Otherwise, we need to perform the adiabatic connection integral within the blue approximation. For $N = 2$ we know the exact result as $\lambda \rightarrow 0$ (exchange limit), where $\tilde{n}_r^{\lambda=0}(\mathbf{r}') = n(\mathbf{r}')/2$, i.e., the conditional probability density is just the density of the remaining electron. By definition, for 2-electrons we have

$$\tilde{v}_s^\lambda(\mathbf{r}'|\mathbf{r}) = v_s[n](\mathbf{r}') - \lambda v_{\text{HX}}[n](\mathbf{r}') - v_C^\lambda[n](\mathbf{r}') + \Delta\tilde{v}_s^\lambda(\mathbf{r}'|\mathbf{r}). \quad (18)$$

In practice, obtaining $v_C^\lambda[n](\mathbf{r}')$ is difficult, and we

approximate

$$\tilde{v}_s^\lambda(\mathbf{r}'|\mathbf{r}) \approx \begin{cases} v_s[n](\mathbf{r}'), \lambda = 0 \\ v[n](\mathbf{r}') + (1 - \lambda)v_{\text{HX}}[n](\mathbf{r}') + \Delta\tilde{v}_s^\lambda(\mathbf{r}'|\mathbf{r}) \end{cases} \quad (19)$$

to recover the exchange limit exactly. In the following calculation for H_2 , we utilize the interpolated blue approximation, Eq. 15, for $\Delta\tilde{v}_s^\lambda(\mathbf{r}'|\mathbf{r})$ and the exact density $n(\mathbf{r}')$ throughout. We obtain an adiabatic connection decomposition for $\lambda \in \{0.0, 0.1, 0.3, 0.5, 0.7, 1.0\}$, and fit the curve to a first-order Padé approximant, which is integrated analytically.

The binding curve for H_2 as a function of bond length is shown in Fig 1(b), and in Table II we present numerical results. In Fig. 3, we show $U_C(R)$ and explain why we chose our interpolation formula as we did. As $R \rightarrow \infty$, any version of the blue electron approximation becomes accurate. To understand this, consider what happens to H_2 as the bond is stretched. The exact wavefunction has Heitler-London [32] form:

$$\Psi^\lambda(\mathbf{r}_1, \mathbf{r}_2) = \frac{1}{\sqrt{2}} (\phi_A(\mathbf{r}_1) \phi_B(\mathbf{r}_2) + \phi_B(\mathbf{r}_1) \phi_A(\mathbf{r}_2)) \quad (20)$$

where ϕ_A and ϕ_B are atomic orbitals localized on each of the two protons. This yields a conditional density:

$$n_r^\lambda(\mathbf{r}') = n_B(\mathbf{r}'), \quad \mathbf{r} \text{ near } A \quad (21)$$

and vice versa, for all $\lambda \neq 0$. Thus the Coulomb energy of the pair density vanishes due to the lack of overlap, and each atomic region yields a one-electron energy of a separate hydrogen atom, the correct answer in this limit. One may consider CP-DFT an exact theory for bond dissociation, unlike the on-top hole theory of Ref. [33], which is not exact.

R	E_X	V_{ee}^{Blue}	U_C^{Blue}	U_C^{Exact}	E_C^{Blue}	E_C^{Exact}
0.0	-1.0245	0.9294	-0.0951	-0.0786	-0.0499	-0.0421
1.0	-0.7472	0.6688	-0.0785	-0.0732	-0.0433	-0.0400
1.4	-0.6619	0.5772	-0.0847	-0.0747	-0.0482	-0.0414
2.0	-0.5698	0.4720	-0.0978	-0.0835	-0.0587	-0.0478
3.0	-0.4775	0.3451	-0.1324	-0.1191	-0.0902	-0.0770
4.0	-0.4323	0.2576	-0.1747	-0.1692	-0.1359	-0.1318
8.0	-0.3749	0.1241	-0.2497	-0.2499	-0.2445	-0.2477

TABLE II. H_2 with bond length R , where E_C^{Blue} is computed from the adiabatic connection using Eq. 19 with the exact density.

Our last 2-electron calculation is for Hooke's atom, two Coulomb repelling electrons in a harmonic potential of force constant k [34]. At $k = 1/4$, the density is known analytically, and at $r = 0$, the exact $\tilde{v}_s^\lambda(\mathbf{r}'|\mathbf{r})$ is radial and can be easily calculated. In Fig. 4 we compare the approximations in Eqs. 14 and 15 with the exact CP

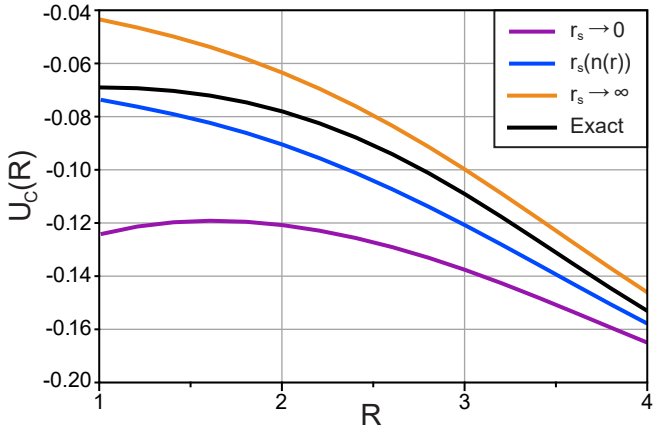


FIG. 3. $U_c(R)$ values from various approximations in H_2 . We plot results from the pure blue electron approximation (Eq. 14, plotted in purple), the interpolated blue electron approximation in the low density limit (Eq. 15 with $n(r) \rightarrow 0$, in orange), the interpolated blue electron approximation (Eq. 15 using exact $n(r)$, in blue), and exact values (in black). The error in the interpolated blue electron approximation never exceeds 20%.

potential and the resulting densities $\tilde{n}_r^\lambda(r')$. Note the accuracy of the blue approximation for large r' , and the cusps as $r' \rightarrow r$ in the exact and approximate CP densities.

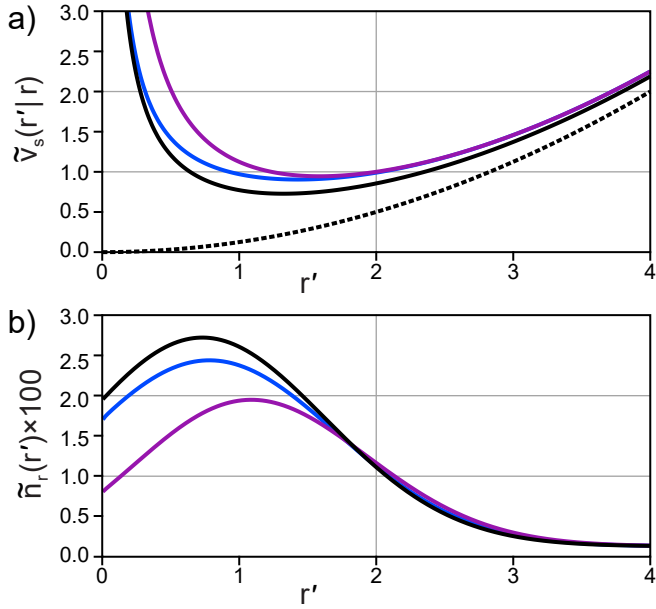


FIG. 4. Hooke's atom. Top: $\tilde{v}_s(r'|r)$ is plotted for the blue interpolation approximation (Eq. 15, plotted in blue), the pure blue electron approximation (Eq. 14, in purple), exactly (in black), and the external potential $r'^2/8$ (black dashed). Bottom: $\tilde{n}_r(r')$ is plotted for the corresponding potentials $\tilde{v}_s(r'|r)$.

Finite temperatures: Possibly, the most important application of CP DFT is for thermal equilibrium in warm

dense matter [9]. While thermal KS-DFT calculations have been very successful, finding consistent temperature-dependent approximations is more difficult than at zero temperature [35], because of the complexity of systems and the cost of accurate quantum chemical simulations. Moreover, calculations using KS solvers eventually fail at extremely high temperatures, due to convergence difficulties with orbital sums.

For finite temperatures, Eq 3 translates to F_{XC} , the XC contribution to the Helmholtz free energy, which folds in entropic contributions [8, 36]. To find accurate CP densities, we solve the KS equations with finite temperature occupations. (We neglect thermal corrections in v_{XC} that have been argued to have relatively little effect on the orbitals [37]). In Fig. 1 (c), we showed results for the potential XC free energy at $r_s = 1.0$ for a wide range of temperatures. The solid line displays the accurate analytical parameterization of Karasiev et al. [16]. The KS CP approximation mildly overestimates f_{XC} for $t = T/T_F$ between about 0.2 and 9, beyond which it fails to converge.

To approach higher temperatures, we performed a much simpler CP calculation using the Thomas-Fermi (TF) approximation [38, 39], often employed in warm dense matter [40, 41], and implementing the simple blue approximation, Eq. 14. We first solved the TF equation at $T = 0$. This was used to initiate iterations for a full numerical solution. We make a simple interpolation of Perrot's [42] accurate parameterization of the Helmholtz free energy density $f_0(n)$ of the uniform non-interacting electron gas constructed to yield the correct $T = 0$ and (classical) $T \rightarrow \infty$ limits:

$$f_0(n) = k_B T n \left(\ln(y) - c + ay^{\frac{2}{3}} \right) \quad (22)$$

where $y = \pi^2 n / \sqrt{2} (k_B T)^{3/2}$, $c = 1 - \ln(2/\sqrt{\pi})$, and $a = 9(2/3)^{1/3}/10$. The Fermi temperature is given by $k_B T_F = (3\pi^2 n)^{2/3}/2$. As $T \rightarrow 0$, $f_0(n) = 3nk_B T_F/5$ as required. TF theory corresponds to minimizing the Mermin [8] grand potential functional ignoring all correlations and making the local density approximation $F[n] = \int d^3r f_0(n(r))$ for the Helmholtz free energy functional of the non-interacting gas. Solving for the CP density, the hole density and XC energies are calculated as previously.

Classical connection: In the classical limit TF theory reduces to the Poisson-Boltzmann (PB) theory used to treat electrical double layers and many other properties of electrolyte solutions and ionic liquids [43]. In the present context the classical analogue of the uniform electron gas is the one-component classical plasma (OCP), namely point charges in a uniform compensating background obeying Boltzmann statistics [43]. In the high temperature limit we can ignore the third term in Eq 22 and the free energy functional of the non-interacting gas reduces to

$$F[n] = k_B T \int d^3r n(\mathbf{r}) \left(\ln \left(\frac{n(\mathbf{r}) \lambda^3}{2} \right) - 1 \right), \quad (23)$$

where $\lambda = (2\pi/k_B T)^{1/2}$ is the thermal de Broglie wavelength of the electron in atomic units. Eq. 23 is identical to the Helmholtz free energy functional of the ideal classical gas, apart from the residual spin degeneracy factor $(2s+1)$. Employing Eq. 23 from the outset corresponds to implementing the classical DFT [43, 44] that generates PB theory for the OCP. We term this the classical approximation CL for the blue electron. It is straightforward to show that in the classical limit the TF screening length, λ_{TF} [45], reduces to the Debye length λ_D of the OCP, given by $(\lambda_D)^{-2} = 4\pi e^2 n/k_B T$.

In Fig. 5 we plot the differences between the results of three different thermal blue-electron approximations and those of Karasiev et al. [16] as a function of $t = T/T_F$, where T_F denotes the Fermi temperature of the bulk. These cover a larger temperature range than in Fig. 1 (c). The blue KS approximation (blue curve) performs quite well across the range. Blue TF (purple curve) overestimates the XC free energy up to $t \approx 10$; for larger values, the various results appear to merge. The classical approximation (green curve) performs surprisingly well for $t > 1$ and this must be exact at sufficiently high t .

In the classical limit (Boltzmann statistics) the CP approach is equivalent to the Percus test particle procedure [13, 43, 46] whereby one fixes a (classical) particle at the origin and measures the one-body density $n(r)$ corresponding to the ‘external’ potential this exerts on the other particles. The bulk (uniform) pair correlation function is given exactly by $g(\mathbf{r}) = n(\mathbf{r})/n_0$, where n_0 is the bulk density. An implementation of the Percus procedure, in the spirit of the present study, is described in a recent classical DFT investigation [47]. There have been several attempts to adapt and exploit the Percus procedure for quantum systems, notably by Chihara [46]. However, the most successful applications relate to liquid metals and electron-ion correlations; see [48] for a summary.

In conclusion, we have presented a non-traditional theoretical approach for extracting XC energies from DFT calculations *without* applying XC functionals for the energy. This conditional probability (CP) DFT is, in principle, exact. CP-DFT calculations require many KS runs for a single system and require a single approximation to the CP potential. But CP-DFT works where DFT with standard approximations fails, and calculations are embarrassingly parallel. A simple interpolation works very well for systems as distinct as the uniform gas and the He atom, neither of which would be regarded as behaving very classically. CP-DFT is exact for one electron, and correctly dissociates H_2 , a system that is widely regarded as being strongly correlated.

The blue-electron approximation becomes exact in many limits: large separations, classical particles, and high temperatures. It may be exact even for strictly correlated electrons, where

$$\tilde{n}_{\mathbf{r}}^{\lambda}(\mathbf{r}') \rightarrow \sum_{j=1}^{N-1} \delta^{(3)}(\mathbf{r}' - \mathbf{f}_j(\mathbf{r})), \quad (24)$$

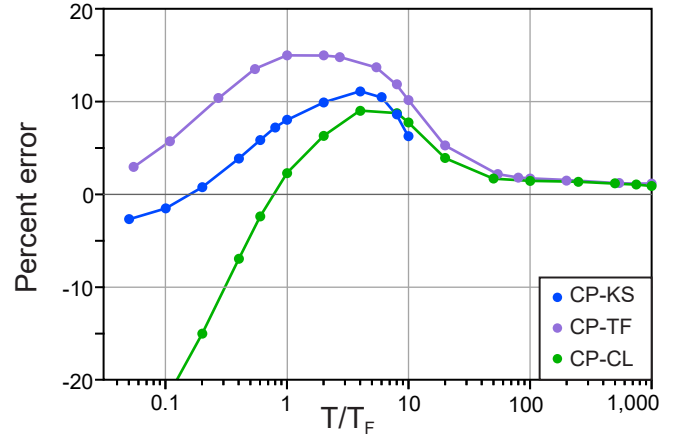


FIG. 5. Percentage error of uniform gas potential XC free energy per electron for the CP-DFT calculations within KS (blue), TF (purple), and classical (green) approximations relative to the parameterization of Karasiev et al. [16]. See Fig. 1 (c) for additional context.

and $\mathbf{f}_j(\mathbf{r})$ is a co-location function [49]. It also becomes increasingly accurate for equilibrium distributions as the temperature increases, becoming exact in the classical limit. Several longer works will follow.

R.J.M. acknowledges funding from the University of California President’s Postdoctoral Fellowship. K.B. and D.P. acknowledge funding from U.S. Department of Energy Grant DE-FG02-08ER46496. R.P. acknowledges U.S. Department of Energy DE-SC0008696. R.E. acknowledges funding from Leverhulme Trust EM 2020-029/4. K.B. thanks John Perdew for suggesting a variation on this project in 1993.

* kieron@uci.edu

- [1] K. Burke, J. Chem. Phys. **136** (2012).
- [2] R. J. Bartlett and M. Musial, Rev. Mod. Phys. **79**, 291 (2007).
- [3] J. Čížek, The Journal of Chemical Physics **45**, 4256 (1966).
- [4] J. B. Anderson, The Journal of Chemical Physics **65**, 4121 (1976).
- [5] B. M. Austin, D. Y. Zubarev, and W. A. Lester, Chemical Reviews **112**, 263 (2012).
- [6] W. Kohn and L. J. Sham, Phys. Rev. **140**, A1133 (1965).
- [7] S. Lehtola, C. Steigemann, M. J. Oliveira, and M. A. Marques, SoftwareX **7**, 1 (2018).
- [8] N. D. Mermin, Phys. Rev. **137**, A: 1441 (1965).
- [9] F. Graziani, M. P. Desjarlais, R. Redmer, and S. B. Trickey, eds., *Frontiers and Challenges in Warm Dense Matter*, Lecture Notes in Computational Science and Engineering, Vol. 96 (Springer International Publishing, 2014).
- [10] M. Bonitz, T. Dornheim, Z. A. Moldabekov, S. Zhang, P. Hamann, H. Kahlert, A. Filinov, K. Ramakrishna, and J. Vorberger, Physics of Plasmas **27**, 042710 (2020), <https://doi.org/10.1063/1.5143225>.
- [11] R. M. Dreizler and E. K. U. Gross, *Density Functional*

Theory: An Approach to the Quantum Many-Body Problem (Springer-Verlag, Berlin, 1990).

[12] M.-C. Kim, E. Sim, and K. Burke, *J. Chem. Phys.* **134**, 171103 (2011).

[13] J. K. Percus, *Phys. Rev. Lett.* **8**, 462 (1962).

[14] K. Burke, J. Perdew, and D. Langreth, *Phys. Rev. Lett.* **73**, 1283 (1994).

[15] J. P. Perdew and Y. Wang, *Phys. Rev. B* **45**, 13244 (1992).

[16] V. V. Karasiev, T. Sjostrom, J. Dufty, and S. B. Trickey, *Phys. Rev. Lett.* **112**, 076403 (2014).

[17] D. Langreth and J. Perdew, *Solid State Commun.* **17**, 1425 (1975).

[18] M. Levy, *Proceedings of the National Academy of Sciences of the United States of America* **76**, 6062 (1979).

[19] E. H. Lieb, *Int. J. Quantum Chem.* **24**, 243 (1983).

[20] K. Burke, J. P. Perdew, and M. Ernzerhof, *The Journal of Chemical Physics* **109**, 3760 (1998).

[21] J. P. Perdew and A. Zunger, *Phys. Rev. B* **23**, 5048 (1981).

[22] M. Levy, J. P. Perdew, and V. Sahni, *Phys. Rev. A* **30**, 2745 (1984).

[23] A. Schild and E. K. U. Gross, *Phys. Rev. Lett.* **118**, 163202 (2017).

[24] S. K. Min, A. Abedi, K. S. Kim, and E. K. U. Gross, *Phys. Rev. Lett.* **113**, 263004 (2014).

[25] S. H. Vosko, L. Wilk, and M. Nusair, *Can. J. Phys.* **58**, 1200 (1980).

[26] J. P. Perdew and Y. Wang, *Phys. Rev. B* **46**, 12947 (1992).

[27] S. R. White, *The Journal of Chemical Physics* **147**, 244102 (2017).

[28] S. R. White and E. M. Stoudenmire, *Phys. Rev. B* **99**, 081110 (2019).

[29] S. R. White, *Phys. Rev. B* **48**, 10345 (1993).

[30] C. Lanczos, *Journal of Research of the National Bureau of Standards* **45**, 255 (1950).

[31] C.-J. Huang and C. J. Umrigar, *Phys. Rev. A* **56**, 290 (1997).

[32] W. Heitler and F. London, *Z. Physik* **44**, 455 (1927).

[33] J. P. Perdew, A. Savin, and K. Burke, *Phys. Rev. A* **51**, 4531 (1995).

[34] S. Kais, D. Herschbach, N. Handy, C. Murray, and G. Laming, *The Journal of chemical physics* **99**, 417 (1993).

[35] T. Dornheim, S. Groth, and M. Bonitz, *Physics Reports* **744**, 1 (2018).

[36] S. Pittalis, C. R. Proetto, A. Floris, A. Sanna, C. Bersier, K. Burke, and E. K. U. Gross, *Phys. Rev. Lett.* **107**, 163001 (2011).

[37] J. C. Smith, A. Pribam-Jones, and K. Burke, *Phys. Rev. B* **93**, 245131 (2016).

[38] L. H. Thomas, *Math. Proc. Camb. Phil. Soc.* **23**, 542 (1927).

[39] E. Fermi, *Zeitschrift für Physik A Hadrons and Nuclei* **48**, 73 (1928).

[40] R. P. Feynman, N. Metropolis, and E. Teller, *Phys. Rev.* **75**, 1561 (1949).

[41] J. Larsen, *Foundations of High-Energy-Density Physics: Physical Processes of Matter at Extreme Conditions* (Cambridge University Press, 2017).

[42] F. Perrot, *Phys. Rev. A* **20**, 586 (1979).

[43] J.-P. Hansen and I. R. McDonald, eds., *Theory of Simple Liquids*, fourth edition ed. (Academic Press, Oxford, 2013).

[44] R. Evans, *Advances in Physics* **28**, 143 (1979).

[45] N. W. Ashcroft and N. D. Mermin, *Solid State Physics*, edited by D. G. Crane (Saunders College Publishing, 1976) p. 826.

[46] J. Chihara, *Journal of Physics: Condensed Matter* **3**, 8715 (1991).

[47] A. J. Archer, B. Chacko, and R. Evans, *The Journal of Chemical Physics* **147**, 034501 (2017), <https://doi.org/10.1063/1.4993175>.

[48] J. A. Anta and A. A. Louis, *Phys. Rev. B* **61**, 11400 (2000).

[49] P. Gori-Giorgi, M. Seidl, and G. Vignale, *Phys. Rev. Lett.* **103**, 166402 (2009).